

# RADIATION ENHANCEMENT AND IMPURITY BEHAVIOR IN JT-60U REVERSED SHEAR DISCHARGES

H. Kubo, S. Sakurai, N. Asakura, K. Shimizu, K. Itami, S. Konoshima, Y. Koide,  
T. Fujita, H. Takenaga, S. Higashijima, K. W. Hill\*

Naka Fusion Research Establishment, Japan Atomic Energy Research Institute,  
Naka-machi, Naka-gun, Ibaraki-ken, 311-0193, Japan

\*Princeton Plasma Physics Laboratory, PO Box 451, Princeton, NJ 08543, USA

## 1. Introduction

The reversed shear plasma is a promising candidate for advanced steady-state tokamak operation. Heat removal by radiation from controlled injection of impurity gases is a useful technique for mitigating the severe problem of concentrated power loading of the divertor [1]. In JT-60U reversed shear plasmas, compatibility between the internal transport barrier (ITB) and a detached divertor plasma has been demonstrated by radiation enhancement using Ne injection [2]. In order to extend such an operation toward high confinement, Ar and Ne have been injected into reversed shear plasmas with high confinement. Radiation enhancement, divertor plasma detachment and impurity behavior have been investigated.

## 2. Experiment

A quasi-steady reversed shear plasma with high confinement ( $H_{89PL} = \tau_E / \tau_E^{89PL} \sim 3.9$ , which was corrected for unconfined orbit loss [3].) has recently been obtained in JT-60U [4]. For such reversed shear plasmas, Ar was injected into the main chamber to enhance the radiation losses [5]. In subsequent experiments, Ne was injected into the divertor to enhance the radiation losses in the divertor plasmas and  $D_2$  was puffed into the main chamber from the top to control the Ne concentration by a puff-and-pump technique [6]. The plasma current was 0.9 - 1.0 MA, toroidal field was  $\sim 3.5$  T, the safety factor at

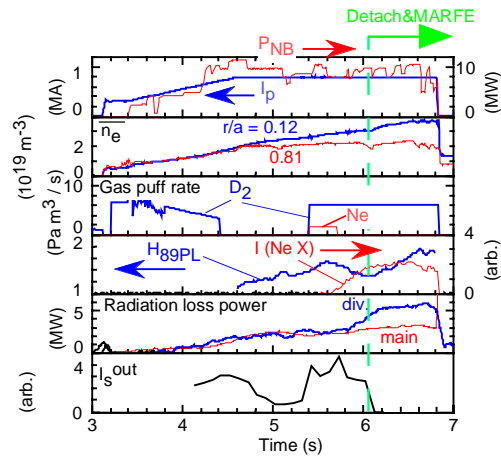


Fig. 1. Waveforms of a reversed shear plasma, where the divertor plasma was detached by Ne injection.  $I_p$ : plasma current,  $P_{NB}$ : NBI power,  $\bar{n}_e$ : line averaged electron densities at  $r/a = 0.12$  and  $0.81$ , gas puff rates of  $D_2$  and Ne,  $H_{89PL}$ ,  $I$  (Ne X): Ne X 1.21 nm line intensity, radiation loss powers from the main and divertor plasmas,  $I_s^{out}$ : ion saturation current at the outer strike point.

the 95% flux surface was 6.1 - 7.1, the elongation was  $\sim 1.4$ , triangularity was  $\sim 0.34$ , and the Greenwald density limit ( $n_{GW}$ ) was  $4.3 - 5.1 \times 10^{19} \text{ m}^{-3}$ . The stored energy was controlled with a feedback technique by changing NBI power in a range of 3 - 14 MW. Waveforms of a reversed shear plasma with Ne injection are shown in Fig. 1.

### 3. Results and discussion

#### 3.1 Radiation enhancement and energy confinement

The  $H_{89PL}$ , ratio of the total radiation loss power ( $P_{rad}^{total}$ ) to the net heating power ( $P_{net}$ ) and ratio of the radiation loss power from the main plasma ( $P_{rad}^{main}$ ) to the total radiation loss power are plotted against the electron density in Fig. 2. With Ar injection, while the electron density increased from  $0.6 n_{GW}$  to  $0.9 n_{GW}$ , the  $H_{89PL}$  decreased from 2.4 to 1.2. Then, while  $P_{rad}^{total} / P_{net}$  stayed around 0.7,  $P_{rad}^{main} / P_{rad}^{total}$  increased from 0.35 to 0.8. The electron temperature at the plasma center decreased from  $\sim 6 \text{ keV}$  to  $\sim 2 \text{ keV}$ . Since some of Ar ions were not fully ionized

in this temperature range, the radiation loss power inside the ITB increased with Ar injection. With Ne injection, high confinement ( $H_{89PL} > 2.4$ ,  $HH_{98(y,2)} = \tau_E / \tau_E^{98(y,2)} > 1.6$  [7]) and high radiation loss ( $P_{rad}^{total} / P_{net} > 0.8$ ) were simultaneously obtained at high density ( $\bar{n}_e > 0.7 n_{GW}$ ). While  $P_{rad}^{total} / P_{net}$  increased,  $P_{rad}^{main} / P_{rad}^{total}$  remained 0.4. Therefore, the radiation loss power from the divertor also increased.

#### 3.2 Divertor plasma detachment

As shown in Fig. 2, at an electron density of  $0.84 n_{GW}$ , the divertor plasma became detached with  $H_{89PL} = 1.8$  ( $HH_{98(y,2)} = 1.2$ ) and  $P_{rad}^{total} / P_{net} = 0.73$ . Figure 1 shows waveforms of the discharge with divertor plasma detachment. Beginning at 4.5 s, the ITB developed, with the electron density in the core region ( $r / a = 0.2$ ) increasing at a faster rate than that in the edge region ( $r / a = 0.8$ ). As shown by the  $H_{89PL}$ ,

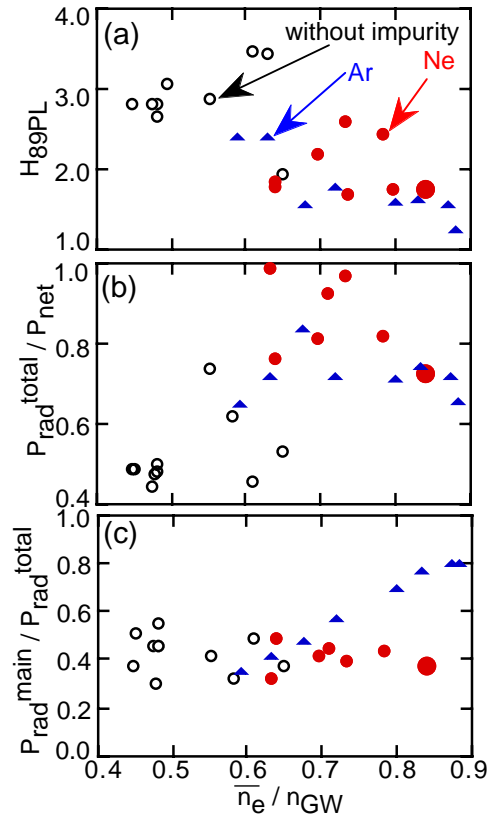


Fig. 2. (a)  $H_{89PL}$ , (b) ratio of the total radiation loss power to the net heating power and (c) ratio of the radiation loss power from the main plasma to the total radiation loss power against the electron density normalized by the Greenwald density limit. The large closed circles indicate a discharge with divertor plasma detachment.

the energy confinement was improved. As the Ne X line intensity increased in the main plasma, the radiation loss power from the divertor increased and a MARFE appeared at the null point. The outer divertor plasma was detached as indicated by a decrease in the ion saturation current. Under conditions of divertor plasma detachment and an X-point MARFE, the  $H_{89pL}$  increased from 1.3 to 1.8. Profiles of the electron temperature, electron density and heat flux at the divertor plates are shown in Fig. 3. After the gas puff, a cold and dense divertor plasma was produced near the inner and outer strike points. Although the detached region was narrow (width  $\sim 1$  cm), the maximum heat flux was greatly decreased by the detachment. Profiles in the main plasma are shown in Fig. 4. The ITB was clearly seen in the profiles of the electron density, ion temperature and electron temperature. The minimum in the safety factor was close to 3. A disruption of the discharge as seen in Fig.

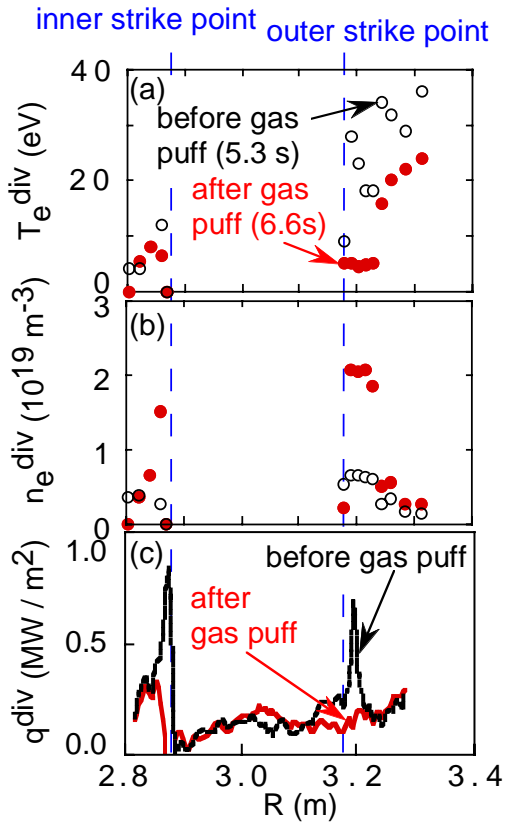


Fig. 3. Profiles of (a) electron temperature, (b) electron density and (c) heat flux at the divertor plates.

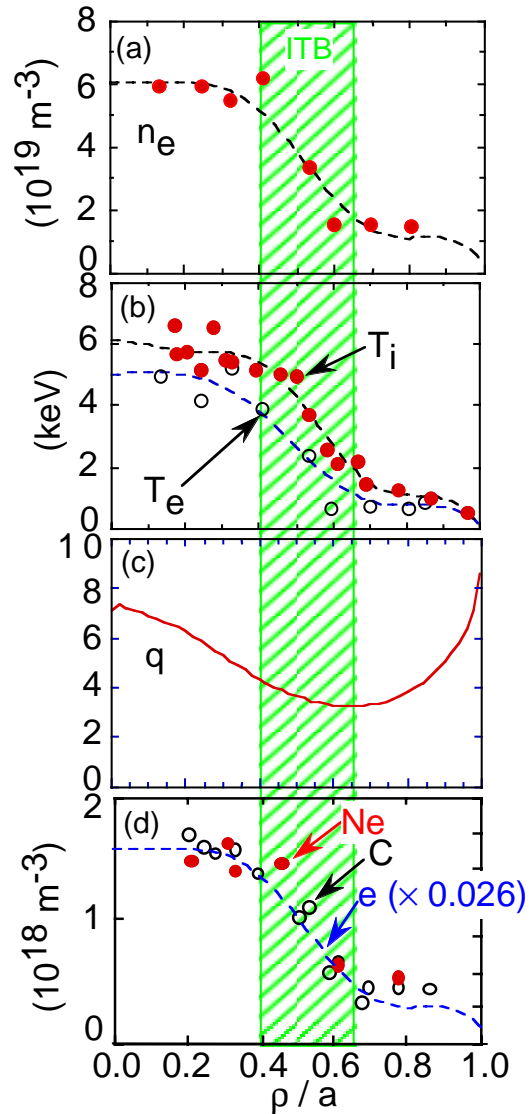


Fig. 4. Profiles of (a) electron density, (b) ion and electron temperatures, (c) safety factor, and (d) Ne, C and electron density in the main plasma with divertor plasma detachment (at 6.6 s in Fig. 1).

1 occurred when the minimum safety factor went through  $q = 3$ .

### 3.3 Impurity behavior

As shown in Fig. 4 (d), the density profiles of Ne and C were similar to that of the electrons. Therefore, impurity accumulation was not significant. From the time evolution of the Ne density profile after Ne injection, it was estimated that the inward velocity and diffusion coefficient at the ITB were  $\sim 3$  m/s and  $\sim 0.5$  m<sup>2</sup>/s, respectively. Using a neoclassical transport calculation code[8], the inward velocity for Ne was estimated to be  $\sim 2$  m/s. Therefore, the experimentally derived inward velocity was consistent with the calculated one. However, the diffusion coefficient was calculated to be  $\sim 0.1$  m<sup>2</sup>/s, which was much smaller than the experimentally derived coefficient.

The Ne X line intensity rolled over around 6.4 s in Fig. 1. However, the time constant of the intensity decrease was long, and the Ne density could not be controlled by pumping.

### 4. Summary

For the reversed shear discharges studied in this paper, in which the electron temperature at the plasma center was  $\sim 6$  keV, Ar injection resulted in radiation loss enhancement inside the ITB. With Ne injection, high confinement ( $H_{89pL} > 2.4$ ,  $HH_{98(y,2)} > 1.6$ ) and high radiation loss ( $P_{rad}^{total} / P_{net} > 0.8$ ) were simultaneously obtained at high density ( $\bar{n}_e > 0.7 n_{GW}$ ). Under conditions of divertor plasma detachment and an X-point MARFE, the ITB became more pronounced and the  $H_{89pL}$  increased from 1.3 to 1.8. The density profiles of Ne and C were similar to that of the electrons, and impurity accumulation was not significant. The effective confinement time for Ne was long, and further enhancement of recycling in the divertor to increase pumping efficiency was necessary for impurity control.

### References

- [1] Kubo, H., et al., Nucl. Fusion **41** (2001) 227.
- [2] Itami, K., et al., Fusion Energy 1997 (Proc. 16th Int. Conf., Montreal, 1996), Vol. 1, IAEA, Vienna (1996) 385.
- [3] Yushmanov, P. N., et al., Nucl. Fusion **30** (1990) 1999.
- [4] Fujita, T., to be published in Fusion Energy 2000 (Proc. 18th Int. Conf., Sorrento, 2000), IAEA, Vienna.
- [5] Sakurai, S., et al., Nucl. Mater. **290-293** (2001) 1002.
- [6] Hosogane, N., et al., Fusion Energy 1998 (Proc. 17th Int. Conf., Yokohama, 1998), Vol. 3, IAEA, Vienna (1999) 903.
- [7] ITER Physics Expert Groups on Confinement and Transport and Confinement Modelling and Database, Nucl. Fusion **39** (1999) 2175.
- [8] Houlberg, W. A., et al., Phys. Plasmas **4** (1997) 3230.